THE ITERATIVE OBJECT SYMMETRY TRANSFORM

*B. Zavidovique**

IEF University of Paris XI
91405-ORSAY, France

V. Di Gesu'

DMA University of Palermo
90123-Palermo, Italy

ABSTRACT

This paper introduces a new operator named the *Iterated Object Transform* that is computed by combining the Object Symmetry Transform with the morphological operator erosion. This new operator has been applied on both binary and gray levels images showing the ability to grasp the internal structure of a digital object. We present some experiments on real images in face analysis.

1. INTRODUCTION

The symmetry is a property that characterizes an *invariance* of a given system. It is one of the most prominent spatial relations perceived by human beings. As for the importance of the concept in machine vision, several surveys have been proposed, a recent quite interesting one being [1]. Symmetry transformations have been suggested in [2, 3] to implement attentive mechanisms in artificial vision systems.

The *Symmetry Axial Transform (SAT)* [4] can be considered one of the first approaches for the detection of symmetry starting from the borders of a digital object. SAT is a subset of the medial axis, derived from the selection of the center of maximal circles for inclusion. SAT is able to retrieve only maximal axes of symmetry, i.e. those symmetries that are already included in the medial axis.

Some limitations of the SAT algorithm have been solved by the introduction of the *Smoothed Local Symmetry* [5]. An innovating approach by Sewisy [6] makes a late avatar of that algorithmic line. Authors couple the Hough transform with geometric symmetry.

In [7, 8, 9] the mathematical background to extract object skewed symmetries under scaled Euclidean, affine and projective images transformation is proposed.

The use of gray level information was firstly investigated in [10]; where the measure of symmetry of a given object is based on a cross correlation operator evaluated on the gray levels. In [11], a local symmetry measure is computed in convolving with the first and second derivative of Gaussians to detect reflectional symmetry.

*This work has been partially supported by the French Ministry of Research and the University Paris XI and MIUR Italian Ministry of Research.

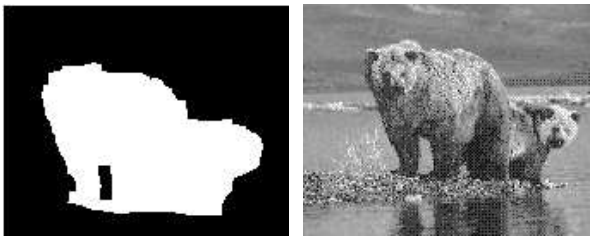

(a) (b)

Fig. 1. Examples of input images: (a) a binary image; (b) a gray level image.

In [12], authors introduce several measures from Marola's one, further extended to finite supports and varying scales for the analysis of object symmetries that are based on the Radon and the Fourier transforms. Scale dependency is considered to detect global symmetries in an image without using any segmentation procedure. Shen and al. [16] detect symmetry in seeking out the lack of it, optimizing a measure comprised of two terms - symmetric and asymmetric.

In [13], the search for symmetries is based on the measure of the *axial moment* of a body around its center of gravity. Gray levels are considered the point masses in the so called *Discrete Symmetry Transform* (DST).

In the following a new operator, the *Iterative Object Transform* (IOT), is introduced. Informally, the IOT is derived by applying iteratively the *Object Symmetry Transform* (S) and the *Erosion* (E) operators in the order. As defined in [13] $S_\theta = \sum g_{i,j}\rho^2_{i,j}$, with $g_{i,j}$ the gray level of pixel (i, j), $\rho^2_{i,j}$ a squared distance from point (i, j) to the axis with slope θ passing through the object center of mass.

In exhibiting symmetries on progressively shrunk versions of an object, the IOT operator allows one to study its inner structures. In fact, its variation (gradient) at successive iterations supports the detection of changes in the object topology or intensity distribution as explained in section 2. The IOT is first tested on regions previously detected. Thanks to a region characterization by *elongation* and *cir-*

cularity, the IOT works for straight symmetric-object detection as well, but the computational complexity still increases due to a loop on the initial object sizes.

The reason why to warp a pattern adaptively in targeting better symmetry evaluation, is that the symmetry of an object may be perceived from its shape (contour) or from its appearance (texture). Then a valid question in building a symmetry detector is as follows: considering that a pattern is a geometric projection of an object onto the focal plane, which importance should be attributed respectively to contours and to texture? Three cases can be distinguished to evaluate the ratio $\frac{S_\theta(X)}{S_\theta(CX)}$, where CX is the contour of X:

1- the silhouette is predominating: then any prior adequate binarization or edge detection would do sending back to the binary pattern situation.

2- interior and edge agree on the axis $r(\theta)$: then a correct estimation of the ratio is obtained again in reducing the grey level distribution to its mean value.

Same as in texture analysis techniques, we assume that the grey-scale can be reduced as some spatial arrangement is accounted for in computing S. Due to the distance (squared) contribution in $S = \sum g_{i,j}\rho_{i,j}^2$, the empty edge axial moment $S_\theta(CX)$ compares to the full axial moment $S_\theta(X)$ like $\sum_{q=1}^{\delta} q^2 = \frac{\delta(\delta+1)(2\delta+1)}{6}$ compares to δ^2, meaning a ratio of $\frac{\delta}{3}$. For a maximum 200 pixel wide object with average grey-level in the 10 −i.e. a 4-bit reduced grey scale− if 255 is assigned to the result of boundary detection then one gets:

full: $S \cong 3\ 10^6$ vs. empty: $S \cong 2.5\ 10^6$
that are pretty comparable.

Note that the assigned label to the contour can be tuned to the expected typical width of symmetric patterns.

3- edges and texture disagree, two more situations:

- if texture is not symmetric then the above ratio decreases along with $S_\theta(X)$ to become in favor of edges.

- if texture is symmetric but in a different direction than edges or if edges are not symmetric at all, (possibly due to numerical truncation, ill-detection etc.), then one could resort to a simple cooperative method *edge-symmetry/region-symmetry* in the fashion of [17], with a loop on the axis direction to check discrepancy.

Rather than strictly this greedy algorithmic line, we adopt here a qualitatively equivalent technique by sequential pattern shrinking. The difference between consecutive eroded versions amounts to edge contribution while all inner subregions are accounted for.

The remaining of the paper is organized as follows. Section 2 provides the definition and formal properties of the IOT. Experimental results and applications are presented in Section 3. Concluding remarks are made in Section 4.

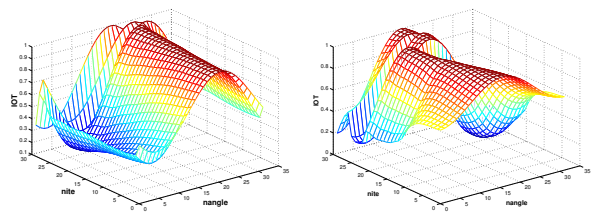

(a) (b)

Fig. 2. Application of the IOT to image in Figure1: (a) binary case; (b) gray level case (x: number of erosions, y: symmetry axis slope, z: symmetry measure).

2. THE ITERATIVE OBJECT TRANSFORM

In the following we describe shortly the IOT. It is performed by applying, in an alternated way, the S operator and a low level operator, erosion E for example, onto the input image, X. Parameters iteratively extracted from this IOT process are suitable for vision (see section 3).

The *Iterated Object Transform*, IOT , is given by:

$$IOT_{\theta,0}(X) = X$$

$$IOT_{\theta,N}(X) = S \circ (E \circ S)_\theta^{n-1}(X) \quad for\ \ n \geq 1$$

where, $\bullet^n$ denotes the application of an operator $\bullet$, n times.

The erosion has been implemented using the min operation [15] on a kernel of size 3×3. The S operator has been implemented computing the normalized axial moments of an object around its center of mass with increments of angle by $\Delta\theta = \frac{\pi}{16}$. This is explained and justified in [13].

In words, the IOT computes the S transform on steadily intensity reduced versions of the input image, until a minimum of intensity is reached. The number of iterations depends on both the size of the input image and the distribution of the gray levels.

Figures 2a,b show the IOT corresponding to input images of bears in Figure 1. The number of iterations depends on both the size of the input image and morphological erosion. The iterative process stops when the percentage of the total intensity of the input image is lower than a given threshold (e.g. 20%).

Starting from the definitions above, the iterated elongation, $\eta_X(n)$, and iterated circularity, $circle_n(X)$, can be introduced as follows:

$$\eta_n(X) = \frac{\min_{\theta\in[0,\phi[}\left\{IOT_{\theta,n}(X)\right\}}{\max_{\theta\in[0,\phi[}\left\{IOT_{\theta,n}(X)\right\}}$$

$$circle_n(X) = 1 - \mathrm{var}\big(IOT_{\theta,n}(X)\ \ for\ \ \theta \in [0,\pi[\big).$$

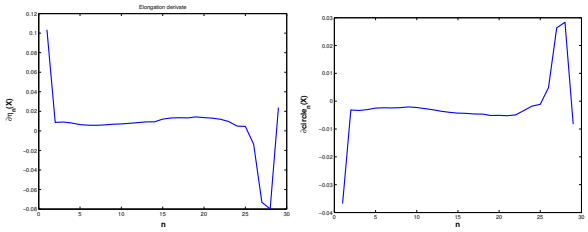

(a) (b)

Fig. 3. Dynamics of the shape parameters in the image Figure 1a: (a) the $\partial\eta_n(X)$; (b) the $\partial circle_n(X)$ function of the number of erosions.

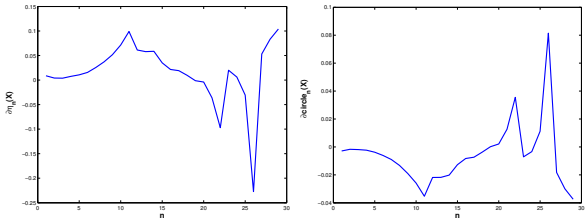

(a) (b)

Fig. 4. Dynamics of the shape parameters in the image Figure 1b: (a) the $\partial\eta_n(X)$; (b) the $\partial circle_n(X)$ function of the number of erosions. The gray level contribution provides for more accurate modelling of likely visual impression.

Figures 3a,b show the shape parameters η_n and $circle_n$ for the images in Figure 1. In case of digital images the $IOT_{\theta,n}(X)$ can be considered as a new image that represents the inner structure of X. The shape operators $\eta_X(n)$ and $circle_n(X)$ exhibit dynamic changes of X shape indicators versus n.

The gradient of the transformations $IOT_{\theta,n}(X)$, $\eta_n(X)$ and $circle_n(X)$ are given by:

$$\partial\big(IOT_{\theta,n}(X)\big) = IOT_{\theta,n}(X) - IOT_{\theta,n-1}(X),$$

$$\partial\big(\eta_n(X)\big) = \eta_n(X) - \eta_{n-1}(X),$$

$$\partial\big(circle_n(X)\big) = circle_n(X) - circle_{n-1}(X).$$

Figures 4a,b show the shape parameters $\partial\eta_n$ and $\partial circle_n$ for the images in Figure 1.

Due to the convolution (linear shift invariant) nature of S, $\partial IOT = S(H(X))$, with $H(X)$ a high pass filtered version of X. Edges on X, $E(X)$, are local maxima of $H(X)$ and then, in the general case $S(E(X)) \neq max(\partial IOT)$. In that respect, η and $circle$ supplement IOT for a more accurate measure of symmetry, taking into account both the inner grey level distribution and the (edge) pattern. The three together allow to determine structural changes in the input image. They indicate the variation of the gray levels distribution inside the object.

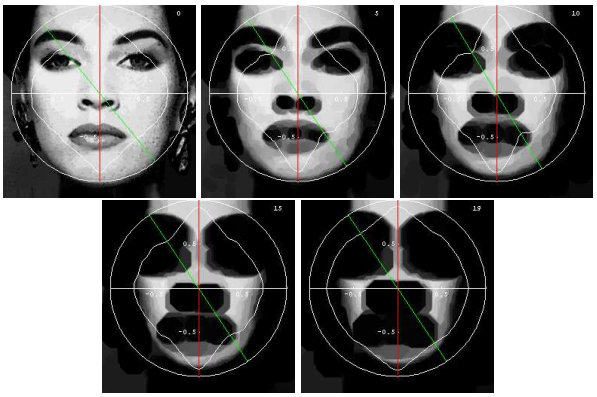

Fig. 5. A sampled sequence of images showing a stable global symmetry.

3. EXPERIMENTAL RESULTS

Artificial images (binary and grey levels) help checking that the IOT is a satisfactory symmetry detector, controlling the coherence of the results and calibrating the method [18]. In the present paper we show results from a second set of experiments carried out on real images - here faces - to show the capability of the IOT in detecting plain objects to contour symmetries, and their variations within the image content. It confirms that the IOT measures some balance between edges and texture symmetry.

The IOT is applied to real images that show evidence of symmetry in given directions. This information may be, for example, useful to detect movements or to determine regularities in an image. In this case the elongation versus the iterations has been considered and plotted in a polar diagram. In the experiment we take angular steps $\Delta\theta = \pi/32$, moreover the erosion is performed alternating the 4-connectivity with the 8-connectivity to obtain the effect of a near circular structuring element. The process stops when the global image intensity is halved. Figure 5 shows a lady with a stable vertical axis of symmetry; the axis with the maximum and minimum elongations are displayed. The sequence of the images is sampled by steps of five iterations starting from the input image. In this example the maximum - vertical - and the minimum - horizontal - axes maintain their directions steadily. This indicates a high degree of symmetry of the pattern and respective to the whole frame too. Actually, in this application the maximum direction indicates the pose

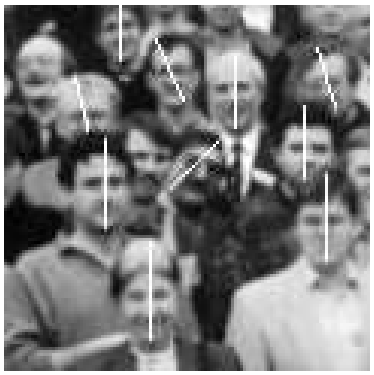

Fig. 6. Extracting faces from their locally stable symmetry.

of the face. Would the lady bend her neck, the maximum direction would stay in agreement with the bending neck for few iterations, well indicating again the pose. But, subsequent iterations would evidence variations due to the asymmetry of the face position respective to the whole frame [18]. That clearly stems from the decreasing importance of the face inner features - symmetric - w.r.t. the global pattern - truncated then asymmetric -. The process was applied to a set of crowd images containing 150 faces to extract them from their peculiar local symmetry axis stability (Figure 6). The success rate is around 80%.

4. FINAL REMARKS

This paper introduces a new class of shape descriptors, in combining morphological operators and symmetry transforms. The evolution of the object symmetry under morphological erosion allows to retrieve information on the object internal structure. This capability helps, in the case of gray level images, to detect the spatial variability of the image intensity. This feature was taken advantage of to improving significantly face pose detection or object classification.

Acknowledgements. The authors thank Cesare Valenti for his help in running programs to experimenting.

5. REFERENCES

[1] David O'Mara, "Automated facial metrology: Symmetry detection and measurement", PhD.Thesis, 2002.

[2] D.Reisfeld, H.Wolfson, H.Yeshurun, "Context free attentional operators: the generalized symmetry transform", *IJCV*, Vol.14, pp.119-130, 1995.

[3] V.Di Gesu', C.Valenti, L.Strinati, "Local operators to detect regions of interest", *Pattern Recognition Letters*, Vol.18, pp.177-181, 1997.

[4] H.Blum and R.N.Nagel, "Shape description using weighted symmetric axis features", *Pattern recognition*, Vol.10, pp.167-180, 1978.

[5] M.Brady, H.Asada, "Smoothed Local Symmetries and their implementation", *The International Journal of Robotics Research*, Vol.3, No.3, pp.36-61, 1984.

[6] A. Sewisy, F. Lebert, "Detection of ellipses by finding lines of symmetry inthe images via an Hough transform applied to staright lines", Image and Vision Computing, Vol. 19 - 12, Oct. 2001, pp. 857-866

[7] D.P.Mukhergee,A.Zisserman,M.Brady, "Shape from symmetry: detecting symmetry in affine images", *London Academy*,Vol.351,pp.77-101,1995.

[8] T.J.Chan, R.Cipolla, "Symmetry detection through local skewed symmetries", *Image and Vision Computing*, Vol.13, No.5, pp.439-455, 1995.

[9] J.Sato, R.Cipolla, "Affine integral invariants for extracting symmetry axes", *Image and Vision Computing*, Vol.15, No.5, pp.627-635, 1997.

[10] G.Marola, "On the detection of the axes of symmetry of symmetric and almost symmetric planar images", *IEEE Trans.of PAMI*, Vol.11, pp.104-108, 1989.

[11] R. Manmatha, H. Sawhney, "Finding symmetry in Intensity Images", Technical Report, 1997

[12] N.Kiryati, Y.Gofman, "Detecting symmetry in grey level images (the global optimization approach)", preprint, 1997.

[13] V.Di Gesu', C.Valenti, "Symmetry operators in computer vision", in *Vistas in Astronomy*, Pergamon, Vol.40, No.4, pp.461-468,1996.

[14] V. Di Gesu', M.C. Maccarone, M. Tripiciano, "Mathematical morphology based on fuzzy operators", *Fuzzy Logic: State of the Art*, R. Lowen and M. Roubens (Eds.), Kluwer Academic, pp.477-486, 1993.

[15] L.Vincent and P.Soille, "Watersheds in digital spaces: an efficient algorithm based on immersion simulations", *IEEE Trans. on PAMI*, Vol.13, N.6, pp.583–598, 1991.

[16] D. Shen, H. Ip, E.K. Teoh, "An energy of assymmetry for accurate detection of global reflexion axes, Image Vision and Computing 19 (2001), pp. 283-297.

[17] D.L.Milgram,"Region extraction using convergent evidence", *CGIP*, Vol.1, pp.1-12, 1979.

[18] B.Zavidovique and V. Di Gesu', "A note on the Iterative Object Symmetry Transform", Tech.Rep.CSG45/02, DMA-Univ.Palermo, 2002.